Vick, Mattrew and Kurt Gramoll, "Finite Element Study on the Optimization of an Orthotropic Composite Toroidal Shell," J. Pressure Vessel Tech, Oct 2012, Vol 134, Issue 5.

Finite Element Study on the Optimization of an Orthotropic Composite Toroidal Shell

Matthew J. Vick
and
Kurt Gramoll
Department of Aerospace and Mechanical Engineering,
University of Oklahoma
865 Asp Ave., Felgar Hall, Rm. 237
Norman, OK 73019
Email: gramoll@ou.edu
Tele: (405) 325-3171

Abstract

Background: In this research an analysis technique is developed to model orthotropic composite toroids and optimize the fiber layup, accounting for the natural variation in thickness due to fiber stacking. The behavior of toroids is difficult to model using membrane shell theories due to a singularity in the strain-displacement relations occurring at the toroid crest that yields discontinuous displacement results.

Method of Approach: A technique is developed here where the constitutive properties of multi-layered toroidal shells are determined using lamination theory and the toroid strains and line loads are determined using finite element analysis. The toroid strains are rotated into the fiber directions, allowing the fiber stress and transverse stress distributions to be determined for each layer. The fiber layup is modified heuristically until an optimum is found. An optimum is reached when the maximum fiber and transverse direction stresses of each shell layer are equal, minimizing wasted fibers and excess weight.

Results: Test cases are analyzed to verify the accuracy of the finite element model and an example composite toroid with Kevlar/epoxy material properties is optimized.
Conclusions: The analysis technique developed here can decrease the time and cost associated with the development of orthotropic toroidal pressure vessels, resulting in lighter, cheaper and more optimal structures. The models developed can be expanded to include a steel liner and a broader range of fiber winding patterns.

Keywords: mechanical engineering, mechanical design, toroid, shell, composite, orthotropic, optimization, finite element, laminate

Introduction

A toroid is an axisymmetric shell of revolution with an arbitrary cross-section that does not intersect the axis of revolution. Toroidal vessels have been used in industry for the storage of pressurized liquids and gases; notable applications include fuel tanks in liquefied petroleum gas (LPG) vehicles and propellant storage in rockets and missiles such as the Russian R-36M ICBM [1]. Toroids offer advantages over other pressure vessel geometries, such as cylinders in certain situations, by providing a more optimal use of space while eliminating wasted material required by end caps.

Vick, Mattrew and Kurt Gramoll, "Finite Element Study on the Optimization of an Orthotropic Composite Toroidal Shell,"
J. Pressure Vessel Tech, Oct 2012, Vol 134, Issue 5.

Manufacturing toroidal pressure vessels using composite materials offers several distinct advantages over more common construction materials like steel, including lighter weight and the ability to tailor the composite material to the design requirements. By varying construction parameters such as fiber orientations for fiber-wound composites, the fiber layup can be optimized to account for the stress variation within the toroid and minimize the weight of the pressure vessel.

Obtaining stress-displacement solutions for toroids is more difficult than other axisymmetric shells of revolution due to a discontinuity occurring in linear membrane solution at the crest of the toroid. Several stress-displacement solutions for internally pressurized isotropic toroids are available in the literature: (a) linear membrane stress approximations [2,3]; (b) closed-form linear displacement solutions [4-8]; (c) numerical stress-displacement solutions based on nonlinear formulations [9,10]; (d) finite element solutions based on modified linear and nonlinear formulations [11-13]. Solutions also exist for orthotropic toroids [14,15], and layup optimization has been considered for fiber-wound toroids [16,17].

These solutions only consider the global behavior of the toroid, neglecting the distributions of fiber direction and transverse direction stresses within each layer of the fibrous composite. A new analysis technique is presented here to evaluate orthotropic toroids and optimize their construction. Tailoring winding patterns to the geometry of the toroid can better control the stress distribution within the toroid, evenly stressing fibers thus reducing the proportion of wasted fibers.

Given an initial fiber layup and toroid geometry, the constitutive properties of the multi-layer toroidal shell are determined using basic lamination theory and calculated using MATLAB, taking into account thickness variations that arise due to fiber buildup. The deformation of the toroid is determined using ANSYS, and the resultant strains and line forces are output for postprocessing. The strains experienced by the toroid are rotated into the fiber direction for each layer, allowing the fiber and transverse direction stresses to be determined for each layer of the toroid.

The aim of the optimization is to produce equal stress distributions in each layer of the toroid, minimizing wasted fibers thus minimizing weight. The fiber layups are modified in an iterative, heuristic process until an optimal fiber layup is reached; optimality is determined using two quantitative fitness measures, the maximum stress in each layer and the ratio of maximum to minimum stress in each layer. Due to the computational efficiency of the model, an optimum can be reached quickly.

Model Formulation

Geometry:

A circular toroid is formed by revolving a circular cross-section with radius a about an axis with major toroid radius R, shown in Fig. 1. The thickness t of the cross-section is usually assumed constant for metallic materials but can vary for orthotropic materials. The meridional direction ϕ for a circular toroid is tangent to the cross-section and the circumferential direction θ

follows the circle of revolution for the toroid. The upper half of the toroid is defined from -90 < ϕ < 90, with the crest occurring at ϕ = 0.

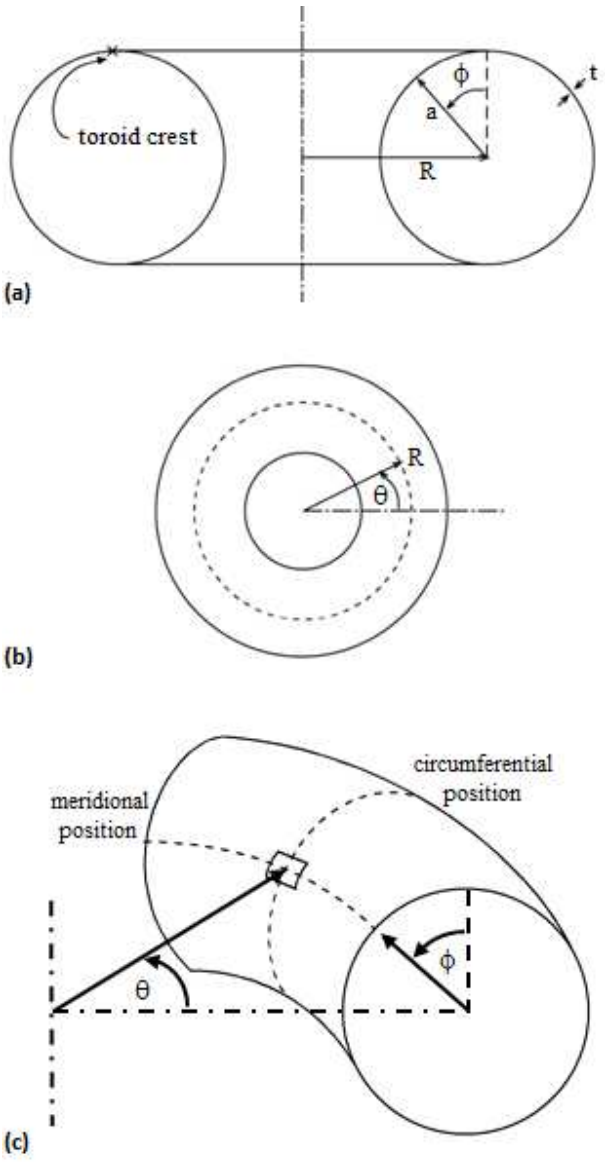

Fig. 1: Circular toroid geometry (a) section view; (b) top view; (c) global view

Due to its geometry, a fiber overwound toroid will have a natural thickness variation due to fiber buildup. The fiber volume is constant across the toroid, thus the thickness of a toroidal shell will decrease radially from the axis of revolution due to the increase in the surface area of the toroid. The shell thickness can be defined as a function of the meridional coordinate, ϕ, and a reference thickness taken to be the thickness at the crest of the toroid, t_c [17]:

$$t(\phi) = \frac{Rt_c}{R - a \cdot \sin\phi} \tag{1}$$

The larger the ratio of toroid cross-section radius to toroid major radius, the more substantial this thickness variation becomes, resulting in greater influence over the stresses and strains experienced by the toroid, shown in Fig. 2:

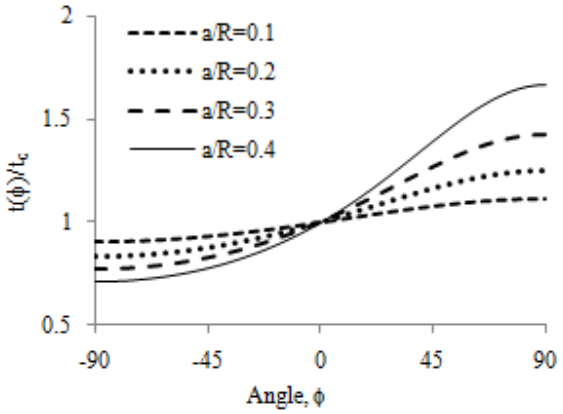

Fig. 2: Thickness variation with meridional position
(normalized with respect to crest thickness, t_c)

Laminate constitutive properties:

For toroids constructed with orthotropic composite materials, the constitutive relationship can be defined using lamination theory, given by [18, 19]:

$$\begin{Bmatrix} N \\ M \end{Bmatrix} = \begin{bmatrix} A & B \\ B & D \end{bmatrix} \begin{Bmatrix} \varepsilon^0 \\ \kappa \end{Bmatrix} \tag{2}$$

where **N** is the vector of in-plane line forces, **M** is the vector of moments per length, $\boldsymbol{\varepsilon}^o$ is the vector of midplane strains, and **κ** is the vector of midplane curvatures. The laminate constant matrices **A**, **B** and **D** correspond to the in-plane stiffness, bending-stretching coupling, and bending stiffness, respectively, defined as [18]:

$$[A] = \sum_{k=1}^{n} \left[\overline{Q}\right]^k \left(z_k - z_{k-1}\right) \tag{3a}$$

$$[B] = \frac{1}{2} \sum_{k=1}^{n} \left[\overline{Q}\right]^k \left(z_k^2 - z_{k-1}^2\right) \tag{3b}$$

$$[D] = \frac{1}{3} \sum_{k=1}^{n} \left[\overline{Q}\right]^k \left(z_k^3 - z_{k-1}^3\right) \tag{3c}$$

for a laminate containing *n*-layers. $\left[\overline{Q}\right]^k$ corresponds to the rotated stiffness matrix of the k^{th} layer of the laminate and z_k corresponds to the distance from the midplane of the laminate to the edge of layer *k*. These matrices differ from other constitutive constants such as Young's modulus owing to the fact they contain geometric information about the laminate carried by the z_k terms.

The bulk engineering constants for a laminate can be determined from the in-plane stiffness matrix **A**. The laminate compliance, **a***, is defined by [18]:

$$\{\varepsilon^0\} = [a^*]\{\bar{\sigma}\} \quad \text{where } [a^*] = \begin{bmatrix} a_{11}^* & a_{12}^* & a_{16}^* \\ a_{12}^* & a_{22}^* & a_{26}^* \\ a_{16}^* & a_{26}^* & a_{66}^* \end{bmatrix} = t[A]^{-1} \tag{4}$$

where $\bar{\sigma}$ is the vector of the average planar stresses. From **a***, the bulk engineering constants for the laminate can be defined [18]:

$$E_x = \frac{1}{a_{11}^*}\ ,\ E_y = \frac{1}{a_{22}^*}\ ,\ \nu_{xy} = \frac{-a_{12}^*}{a_{11}^*}\ ,\ \nu_{yx} = \frac{-a_{12}^*}{a_{22}^*}\ ,\ G_{xy} = \frac{1}{a_{66}^*} \tag{5 a, b, c, d, e}$$

As all fibers are oriented within the plane of the laminate, the constants defining behavior through the thickness of the laminate, E_z, ν_{xz}, and G_{xz}, are defined using the fiber and matrix properties of the laminate and are independent of fiber orientation.

Finite element models

ANSYS offers a variety of tools that aid in the analysis of orthotropic shells, most importantly shell elements that allow axisymmetric modeling and material properties to be input as preintegrated shell sections using laminate constants. ANSYS provides several built-in shell elements for structural analysis; two elements used in this analysis are SHELL209 and SHELL281. SHELL209 is a one-dimensional, three-node finite strain axisymmetric shell element that requires the cross-section of the toroid to be modeled in the x-y plane using lines; the y-axis serves as the axis of revolution. SHELL281 is a two-dimensional, eight-node finite strain shell element that requires a three-dimensional model of the toroid; the toroid can be modeled by the cross-section swept through a small arc with axisymmetric boundary conditions applied to the free edges of the sweep. SHELL281 is one of two ANSYS shell elements that allows material and thickness data to be applied as preintegrated shell sections; for this reason it is the main element used in this analysis.

When utilizing preintegrated shell sections for composite layups, ANSYS requires the values of the **A**, **B**, and **D** matrices of the laminate to be input along with values of an **E** matrix that defines shear behavior through the thickness of the laminate. The **E** matrix is specified by ANSYS as [20]:

$$[E] = \frac{5}{6}\begin{bmatrix} G_{xz}t & 0 \\ 0 & G_{xz}t \end{bmatrix} \tag{6}$$

Layer stresses

When considering composite shells, it is convenient to output the element line forces and element planar strains for further postprocessing. Planar strains allow simple rotations to determine fiber direction and transverse direction stresses in individual layers (transverse stress through the thickness of the shell is negligible for shell formulations). Utilizing the planar

strains, ε_1 (meridional strain), ε_2 (circumferential strain), and ε_{12} (planar shear strain), output by ANSYS, the stress state of each layer of the shell is determined by [18]:

$$\{\bar{\sigma}\} = [Q]\{\bar{\varepsilon}\} \text{ where } \{\bar{\varepsilon}\} = \begin{bmatrix} m^2 & n^2 & mn \\ n^2 & m^2 & -mn \\ -2mn & 2mn & m^2 - n^2 \end{bmatrix} \begin{Bmatrix} \varepsilon_1 \\ \varepsilon_2 \\ \varepsilon_{12} \end{Bmatrix} \tag{7}$$

Q is the layer stiffness matrix, $\bar{\varepsilon}$ is the layer strain rotated by α_k from the global coordinate system (Fig. 3) into the direction of the fiber, $m = \cos(\alpha_k)$ and $n = \sin(\alpha_k)$. Equation (7) directly gives the fiber direction and transverse direction stresses within each layer, allowing a comparison of stress states within each layer through the cross-section of the toroid and providing the basis of the layup optimization process.

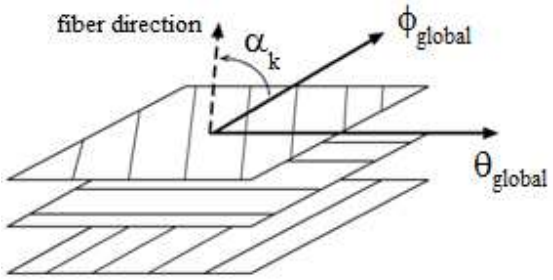

Fig. 3: Laminate fiber orientations

Model Verification

Three models and three test cases are considered to verify the accuracy and consistency of the finite element formulations for internally pressurized toroids. Models include:

a) two-dimensional axisymmetric finite element formulation with material properties defined by engineering constants and individually defined element thicknesses
b) two-dimensional axisymmetric finite element formulation with material properties defined by engineering constants and element thicknesses defined by a global function using the SECFUNCTION command in ANSYS
c) three-dimensional axisymmetric finite element formulation with material properties defined by preintegrated shell sections
d)

Test cases include:

a) isotropic toroid with constant thickness
b) isotropic toroid with variable thickness
c) orthotropic toroid with variable thickness

Each finite element model is based upon a circular cross-section of the toroid. The cross-section is constructed using 360 line arcs each spanning one degree, thus forming a complete circle. For two-dimensional models, the lines are directly meshed into elements; for three-dimensional models, the lines are revolved one degree to form areas which are meshed into elements. Each model contains 360 elements. Pressure loads are applied directly to element

faces using 10 sub-steps to account for possible nonlinear deformation. The y-displacement of nodes at ϕ = 90° are constrained to be zero and results are determined using the default nonlinear solver within ANSYS.

Isotropic, constant thickness toroid

An isotropic toroid with parameters R = 15 in (381 mm), a = 10 in (254 mm), t = 0.5 in (12.7 mm), E = 10 Msi (68.9 GPa), ν = 0.3, p = 1000 psi (6.89 MPa) is considered for the first test case. Two finite element models are considered: a two-dimensional model with constitutive properties defined as engineering constants referred to as EC (for *engineering constants*) with thickness defined for each element individually, and a three-dimensional model with constitutive properties defined as laminate constants referred to as PI (for *preintegrated shell sections*).

This toroid configuration has been analyzed by Tielking et al [11] using MLT (*modified linear theory*) with published stress and displacement results. Figure 4 presents displacement and normalized line force results for the toroid (displacement is shown at 100 times actual magnitude for clarity). The center of the toroid cross-section is given by x = 0 and the line force resultants are normalized by $p \cdot a$ and presented as a function of meridional position, ϕ. There is good agreement between the displacements predicted by MLT and EC, and the in-plane strain and line force results obtained from EC and PI are identical.

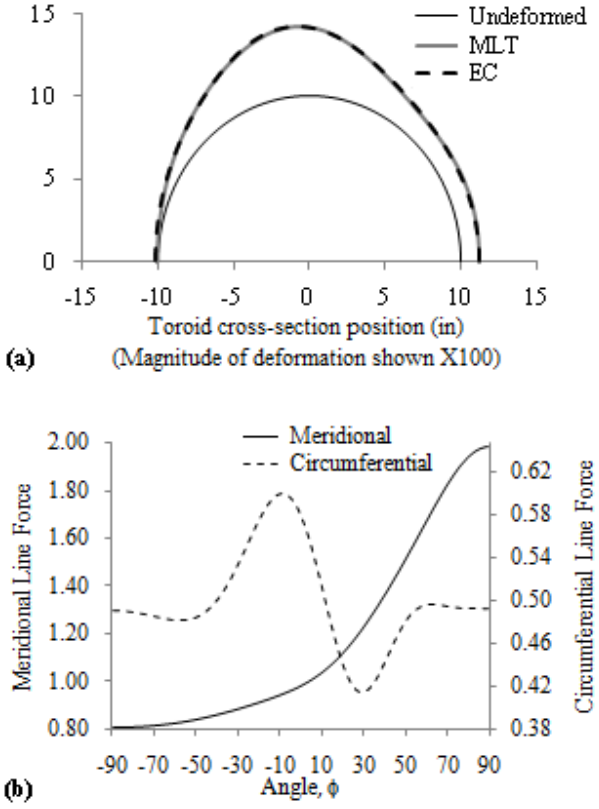

Fig. 4: Isotropic, constant thickness toroid (a) toroid displacement comparison; (b) FEA normalized line forces (EC and PI results identical)

Isotropic, variable thickness toroid

No satisfactory explicit solution exists in the literature for an isotropic toroid of variable thickness; for this case, two different finite element models are compared to ensure consistency of results. The first finite element model is a two-dimensional model referred to as EC where the toroid shell thickness is defined as a global function utilizing the ANSYS command SECFUNCTION. The second finite element model is a three-dimensional model referred to as PI; the shell thickness is defined implicitly for each element in this model by the preintegrated shell constants.

The toroid considered for this case has parameters R = 15 in (381 mm), a = 10 in (254 mm), E = 10 Msi (68.9 GPa), ν = 0.3, p = 1000 psi (6.89 MPa). The shell thickness of the toroid is defined by Eq. (1) where the thickness at the crest is given by t_c = 0.75 in (19.05 mm). This function leads to a large variation in shell thickness, ranging from 0.45 in (11.43 mm) at the outside of the toroid to 2.25 in (57.15 mm) at the inside of the toroid, five times the outside value.

The meridional, ε_Φ, and circumferential, ε_θ, strain resultants for the two models are in good agreement (Fig. 5a) and the resultant line forces are identical (Fig. 5b) despite the significant differences in finite element formulation. Additionally, the resultant line forces for both the constant thickness toroid and variable thickness toroid are similar, which is to be expected given the identical toroid cross-section geometries.

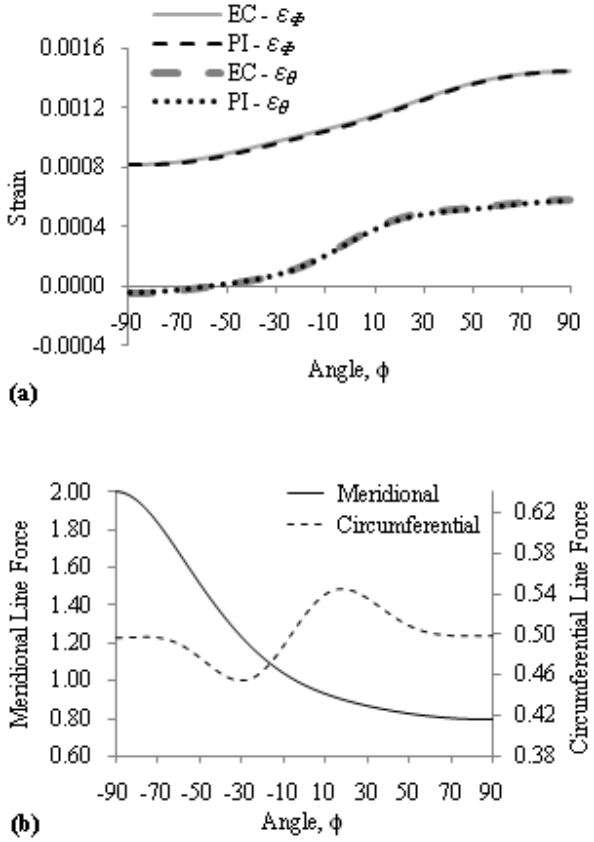

Fig. 5: Isotropic, variable thickness toroid (a) planar strains;

(b) normalized line forces (EC and PI results identical)

Orthotropic, variable thickness toroid

For orthotropic models, the toroid shell thickness is defined for each element individually. The meridional direction is denoted by a subscript 1, the circumferential direction is denoted by a subscript 2, and the through-plane direction is denoted by a subscript 3. Two finite element models are considered, a two-dimensional model utilizing engineering constants (EC) and a three-dimensional model utilizing preintegrated shell sections (PI). The toroid considered has geometry R = 15 in (381 mm), a = 10 in (254 mm) and has a thickness function defined by Equation (1) where t_c = 0.75 in (19.05 mm).

The orthotropic material properties are defined to be E_1 = 10 Msi (68.9 GPa), $E_2 = E_3$ = 5 Msi (34.5 GPa), v_{12} = 0.3, v_{23} = 0.37, G_{12} = 0.3 Msi (2.07 GPa), G_{23} = 0.2 Msi (1.38 GPa). The material properties are arbitrary and are considered to be the bulk engineering constants for a laminate. When calculating the **A**, **B**, **D**, and **E** matrices, each lamina is assumed to already be oriented in the global coordinate system.

The resultant line forces for EC and PI are identical and the strain resultants for the two models are in good agreement (Fig. 6). The finite element analyses produce consistent, logical results, establishing confidence in the validity of the finite element models applied to orthotropic toroids with variable thickness.

Vick, Mattrew and Kurt Gramoll, "Finite Element Study on the Optimization of an Orthotropic Composite Toroidal Shell,"
J. Pressure Vessel Tech, Oct 2012, Vol 134, Issue 5.

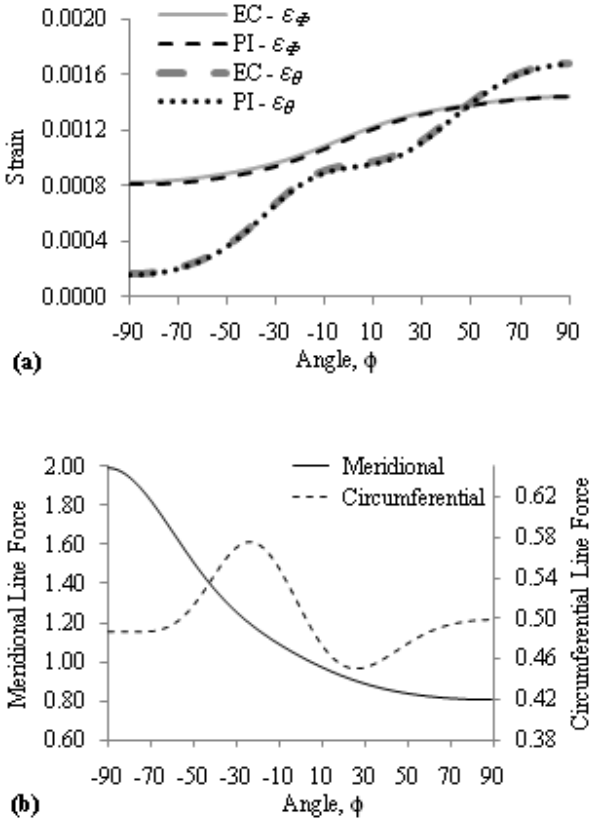

Fig. 6: Orthotropic, variable thickness toroid (a) planar strains;
(b) normalized line forces (EC and PI results identical)

Toroid Layup Optimization

Optimizing the toroid layup requires a systematic approach and quantitative measures of fitness with which to compare the layups. In this study the layups are optimized heuristically and layup fitness is measured by the maximum stresses within each layer and the evenness of the stress distribution within each layer given by the ratio of the maximum stress to minimum stress within the layer. The model is optimized using stresses instead of failure criteria to allow broader applicability; in the event failure strengths of the composite are unknown the model can still be used for basic optimization. In order to account for possible large deformations, the finite element models used in the optimization are solved using basic nonlinear analysis in ANSYS by dividing the applied load into ten equal load steps and assuming deformation is linear in each step. The optimization process is described in Fig. 7:

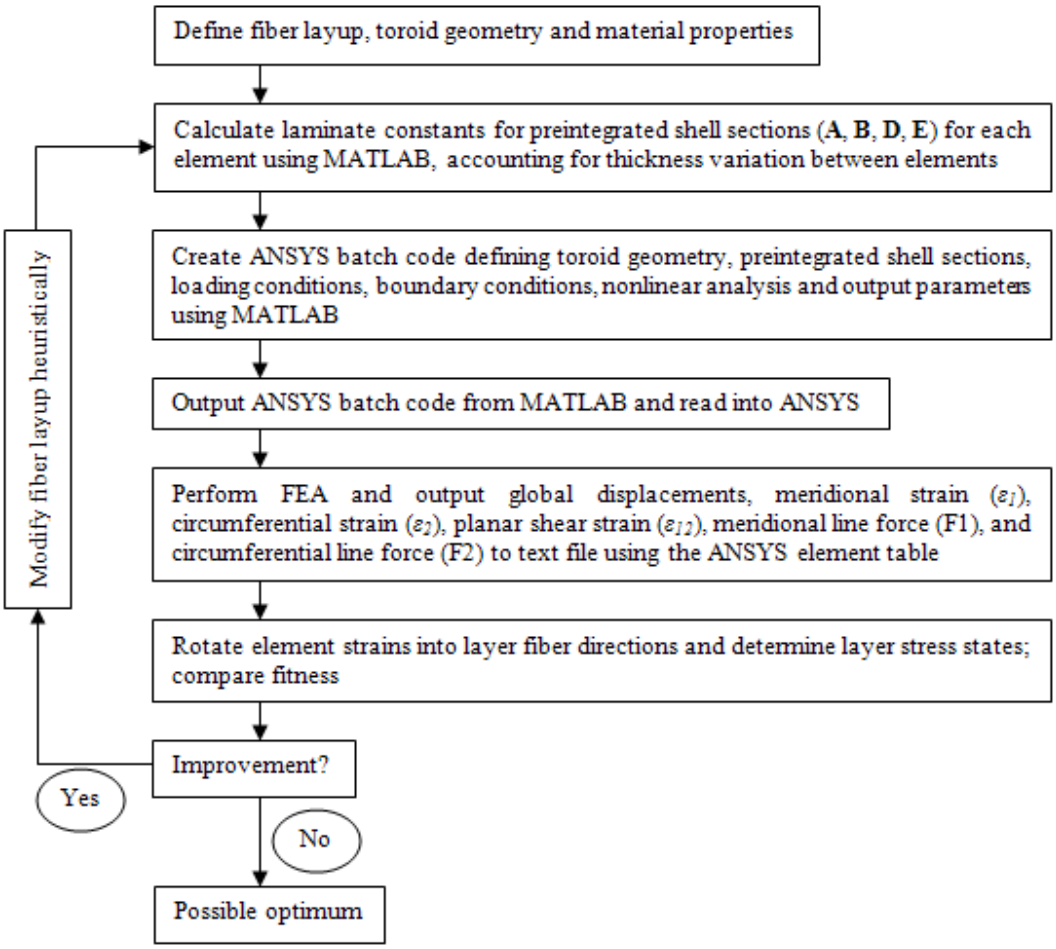

Fig. 7: Heuristic optimization process

Example: Kevlar/epoxy toroid

The toroid considered for optimization has geometry R = 15 in (381 mm), a = 10 in (254 mm), and is subject to an internal pressure p = 1000 psi (6.895 MPa). The toroid is constructed using a Kevlar/epoxy composite with material properties given in Table 1. The toroid constitutive properties are defined in ANSYS using preintegrated laminate constants.

Table 1: Kevlar/epoxy material properties [18]

Parameter	**Value**
E_1	11 Msi (76.8 GPa)
$E_2 = E_3$	0.8 Msi (5.5 GPa)
ν_{12}	0.34
ν_{23}	0.37
G_{12}	0.3 Msi (2.07 GPa)
G_{23}	0.2 Msi (1.4 GPa)

Axial tensile strength	200 ksi (1380 MPa)
Transverse tensile strength	4 ksi (27.6 MPa)
Ply thickness	0.005 in (0.127 mm)

Fiber layups are restricted to four layer repeated unit cell patterns and are denoted $[a / \pm b / c]_n$ where a, b, and c are the fiber orientation angles. This unit cell layup is repeated until the predefined toroid thickness is reached. It is assumed that these fiber orientations remain constant around the cross-section of the toroid; that is each element of the toroid has the same fiber orientations. An orientation in the 0 direction is defined to follow the meridional direction of the toroid and a 90 orientation is defined to follow the circumferential direction of the toroid (Fig. 8).

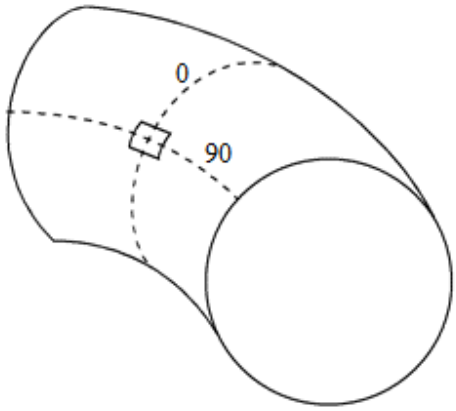

Fig. 8: Fiber layup orientations

Due to the symmetry of the toroid, two of the layers in the pattern are restricted to be angle-ply, denoted by ±b. As the principal stresses within the toroid lie in the meridional and circumferential directions, it is helpful to define layer *a* to be 0 and layer *c* to be 90. For layers oriented at 90, there is no fiber buildup. To account for this, the shell thickness function from Eq. (1) is applied to individual lamina ($t_l = 0.005\ in$) with orientations other than 90, allowing the overall shell thickness and proper preintegrated shell constants to be calculated. The total toroid crest thickness, t_c, is defined to be 0.75 in.

For the given toroid geometry, the maximum fiber and transverse stresses within each layer appear to converge to a single value for an angle-ply near 9 degrees off the meridian, shown in Fig. 9. This convergence is interesting for two reasons: (a) the large number of unalterable variables (thickness variation, variation in meridional and circumferential loads) affecting the stress within the toroid; (b) it corresponds to the overall minimum of the maximum stresses within the toroids. In other words, every other fiber orientation results in a higher maximum stress in some layer within the toroid. It is also interesting that the same layup is optimum for both the fiber direction and transverse direction stresses. The relationship between

the fiber stress and the angle-ply is inverted for the transverse stress, which is logical; a fiber rotation that causes an increase in stress within that fiber will cause a corresponding decrease in transverse stress given a constant loading. Planar shear stresses were calculated but not considered in the optimization; shear stresses were around 2 orders of magnitude smaller than circumferential stresses and 3 orders of magnitude smaller than meridional stresses in all cases analyzed.

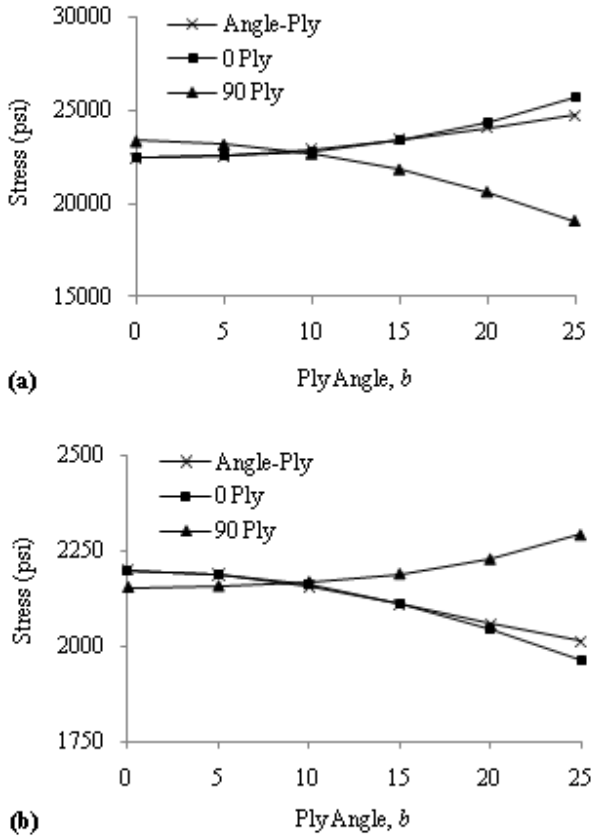

Fig. 9: Maximum layer stresses with respect to angle ply orientation
(a) fiber direction; (b) transverse direction

To examine the evenness of the stress distributions through the toroid, the ratios of the maximum to the minimum stress within each layer for each layup are plotted in Fig. 10. Each stress state oriented along the meridional direction (fiber directions near 0 and transverse directions near 90) experiences a relatively constant stress ratio between 1.8 and 1.9 owing to the relatively invariant nature of the meridional line load (refer to Fig. 4, Fig. 5 and Fig. 6). There is a notable variation in the stress ratio for stress states oriented along the circumferential direction, with the ratio increasing as the angle-ply layers rotate further from the meridional direction. The stress ratio is relatively constant for angle-ply rotations less than 10, and the stress ratio tends to increase as the angle-ply orientation increases, thus a fiber layup with an angle-ply orientation near 9 remains optimal.

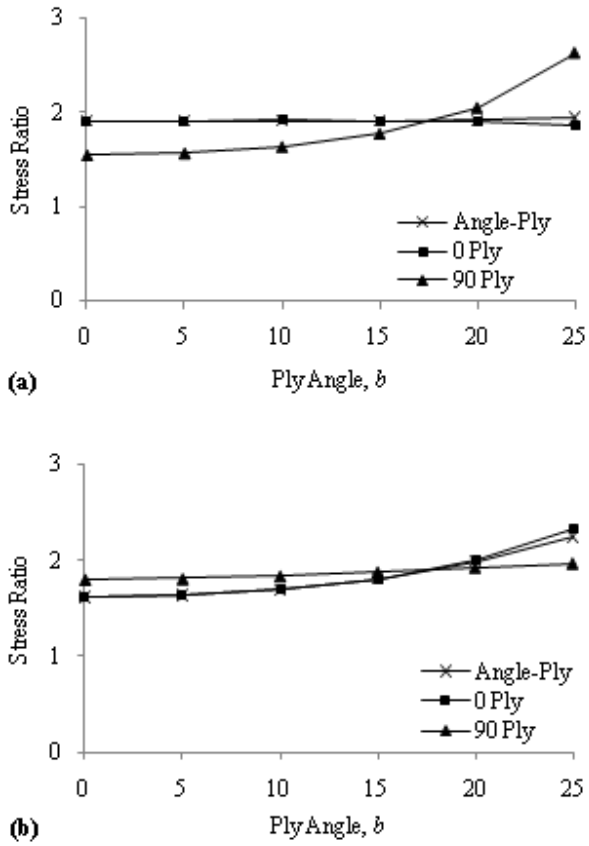

Fig. 10: Ratio of maximum to minimum layer stresses with respect to angle-ply orientation
(a) fiber direction; (b) transverse direction

Summary and Conclusions

Several advancements have been made in optimizing composite toroids, including a new axisymmetric, large deformation finite element model in which MATLAB is used to calculate the laminate properties for individual shell element comprising the toroid, ANSYS is used to determine the planar strains of each element, and the strains are rotated to determine the fiber direction and transverse direction stresses within each layer of the toroid. These stresses are used to heuristically optimize the toroid such that there is an even stress distribution within the toroid, minimizing the amount of wasted fibers in the toroid thus minimizing the weight of the toroid.

Though only four-layer unit cell fiber layups are considered here, the model can easily be expanded to include a wide variety of layups including geodesic windings, prepreg laminates and the addition of a metal liner. Determining the effects of such discontinuities such as nozzles is currently out of the scope of this model.

References

[1] Podvig, P., Bukharin, O., Hippel, F., 2004, *Russian Strategic Nuclear Forces*, MIT Press, Cambridge, Massachusetts, pp. 214-215, Chap. 4.

[2] Timoshenko, S., Woinowsky-Kreiger, S., 1959, *Theory of Plates and Shells*, McGraw-Hill, New York, New York, Chap. 14.

[3] Ugural, A., 1999, *Stresses in Plates and Shells*, McGraw-Hill, New York, New York, Chap. 12.

[4] Dean, W. R., 1939, "The Distortion of a Curved Tube due to Internal Pressure", Philosophical Magazine, **28**(189), pp. 452-464.

[5] Clark, R. A., 1950, "On the Theory of Thin Elastic Toroidal Shells", Journal of Mathematics and Physics, **29**(3), pp. 146-178.

[6] Kydoniefs, A. D., Spencer, A. J., 1967, "The Finite Inflation of an Elastic Toroidal Membrane of Circular Cross Section", International Journal of Engineering Science, **5**(4), pp. 367-391.

[7] Kydoniefs, A. D., 1967, "The Finite Inflation of an Elastic Toroidal Membrane", International Journal of Engineering Science, **5**(6), pp. 477–494.

[8] Ren, W., Liu, W. Zhang, W., Reimerdes, H. G., Oery, H., 1999, "A Survey of Works on the Theory of Toroidal Shells and Curved Tubes", Acta Mechanica Sinica, **15**(3), pp. 225-234.

[9] Jordan, P. F., 1962, "Stresses and Deformations of the Thin-Walled Pressurized Torus", Journal of the Aerospace Sciences, **29**(2), pp. 213-225.

[10] Sanders, J. L., Liepins, A. A., 1963, "Toroidal Membrane under Internal Pressure", AIAA Journal, **1**(9), pp. 2105-2110.

[11] Tielking, J. T., McIvor, I. K., Clark, S. K., 1971, "A Modified Linear Membrane Theory for the Pressurized Toroid", Journal of Applied Mechanics, **38**(2), pp. 418-422.

[12] Hinton, J., Sienz, J., Özakça, M., 2003, *Analysis and Optimization of Prismatic and Axisymmetric Shell Structures*, Springer, London, United Kingdom, Chap. 4.

[13] Papargyri-Beskou, S., 2005, "Finite-element analysis of an axisymmetric, thin-walled, nonlinear elastic pressurized torus", Acta Mechanica, **178**, pp. 1-22

[14] Clark, S. K., Budd, C. B., Tielking, J. K., 1972, "Tire Shape Calculations by the Energy Method", Kautschuk und Gummi, Kunststoffe, **25**(12), pp. 587-596.

[15] Maksimyuk, V. A., Chernyshenko, I. S., 1999, "Nonlinear Elastic State of Thin-Walled Toroidal Shells Made of Orthotropic Composites", International Applied Mechanics, **35**(12), pp. 1238-1245.

[16] Marketos, J. D., 1963, "Optimum Toroidal Pressure Vessel Filament Wound Along Geodesic Lines", AIAA Journal, **1**(8), pp. 1942-1945.

[17] Li, S., Cook, J., 2002, "An Analysis of Filament Overwound Toroidal Pressure Vessels and Optimum Design of Such Structures", Journal of Pressure Vessel Technology, **24**(2), pp. 215-222.

[18] Herakovich, C. T., 1998, *Mechanics of Fibrous Composites*, John Wiley and Sons, Inc., New York, New York, Chap 5.

[19] Tsai, S. W., Hahn, H. T., 1980, *Introduction to Composite Materials*, Technomic Publishing Company, Westport, Connecticut, Chap 4-6.

[20] ANSYS, Inc., "Release 11.0 Documentation for ANSYS"